SIAM J. CONTROL OPTIM.
Vol. 60, No. 5, pp. 3127–3147

MULTIVARIATE ESTIMATOR FOR LINEAR DYNAMICAL SYSTEMS WITH ADDITIVE LAPLACE MEASUREMENT AND PROCESS NOISES*

NHATTRIEU C. DUONG†, JASON L. SPEYER†, AND MOSHE IDAN‡

Abstract. Since uncertainties in many physical systems have impulsive properties poorly modeled by Gaussian distributions, heavier-tailed distributions, such as Laplace, may be used to improve model characteristics. From insights obtained through development of the scalar Laplace estimator, an algorithm is determined for the vector-state case. For a discrete-time vector linear system with scalar additive Laplace-distributed process and measurement noises, the a priori and a posteriori conditional probability density functions (pdfs) of the system states given the measurement history are propagated recursively and in closed form. The conditional pdfs are composed of signs and absolute values of affine functions, and a basis composed of signs of affine functions is constructed to simplify their representation. The a posteriori conditional mean and variance are derived analytically from the conditional pdf using characteristic functions. Generalization to independent vector measurement and process noises is straightforward. From the general method for deriving Laplace estimators in n-dimensions, a two-dimensional minimum variance estimator is explicitly developed, and a simulation is presented.

Key words. Laplace, estimation, stochastic, linear, systems

MSC code. 93E10

DOI. 10.1137/21M1391237

1. Introduction.

In many engineering applications, random processes or noises have volatility that are not well modeled by Gaussian distributions. The Gaussian distribution is considered a light-tailed distribution, whose tails decay at an exponential rate or faster [2]. While its structure lends itself to compact, closed-form analytical results, this is, in fact, a constraint on the robustness of its modeling. The light tails poorly model systems with noise spikes, such as radar, sonar [15], and stock market volatility [17], and algorithms built on Gaussian distributions are susceptible to such outliers. While ad hoc methods, such as prefilters, have been developed to compensate for this limitation, we instead wish to exploit the properties of the Laplace distribution for this purpose.

With the advent of fast, inexpensive computational capabilities, simulation methods have been used to fill in the gap where analytical filters have been absent. Particle filters have had widespread use in nonlinear systems [18] in robotics [14], navigation, and image processing, using both Gaussian and non-Gaussian noises. Laplace densities have been used in areas such as image [19] and speech [16] processing. Additional prior work has included the estimation of a Laplace random vector corrupted by Gaussian noise [21] and state estimation for linear systems driven by Laplace noise using a bank of Kalman filters [8]. However, these techniques are approximate by nature and do not produce explicit closed-form expressions for the minimum variance

*Received by the editors January 19, 2021; accepted for publication (in revised form) March 21, 2022; published electronically October 13, 2022.
https://doi.org/10.1137/21M1391237
Funding: This material is based on work supported by the National Science Foundation under grants NSF/ENG/ECCS-BSF, 1607502, and 1934467, as well as by the United States – Israel Binational Science Foundation (BSF) joint NSF-BSF ECCS program under grants 2015702 and 2019639.
†Department of Mechanical and Aerospace Engineering, University of California, Los Angeles, Los Angeles, CA 90095 USA (ncduong@ucla.edu, speyer@seas.ucla.edu).
‡Faculty of Aerospace Engineering, Technion, Haifa 32000, Israel (moshe.idan@technion.ac.il).

estimate.

When the state and noise are both Gaussian, Cauchy, or Laplacian, there is a closed-form solution. In any other case, a closed-form solution is not known, and numerical ad hoc cost criteria are constructed and numerical optimization techniques are then applied [3, 13]. In this paper, if static measurements are considered where both the state and additive noise are Laplacian, the conditional probability density function (pdf) is obtained in closed form and the minimum error variance estimate, the conditional mean, is also obtained in closed form. Since our objective is to construct dynamic state estimators where the state dynamic system is linear with additive Laplacian process noise, this static result is generalized in that the conditional pdf is constructed analytically and recursively through both measurement updates and dynamic propagation. There are no approximations and no ad hoc optimizations. Once one has an analytic conditional pdf, the associated statistics can also be determined analytically. This is the essence of our contribution.

Past efforts in deriving analytic recursive estimators for discrete-time linear vector state systems other than the Gaussian (Kalman) filter have used Cauchy distributions, whose heavy tails better capture volatile phenomena [10, 11, 12, 9]. The development of a recursive, analytic filter based on Cauchy uncertainties required that the derivation be structured using characteristic functions of unnormalized conditional pdfs of the state given a measurement sequence. For brevity, these will be simply referred to as conditional pdfs going forward. In this formulation, the characteristic functions are functionally similar to the Laplace pdfs. Therefore, many of the analytic techniques that were developed for the characteristic functions are applicable, in modified form, for deriving the Laplace estimator. In contrast to the Cauchy pdfs, the Laplace densities, whose tails decay exponentially although at a slower rate than the Gaussian densities, have well-defined moments. Whereas the argument of the Gaussian exponential is L_2, the argument of the Laplace exponential is L_1, which produced in the scalar Laplace system estimates that were significantly different from those that would be generated from a Gaussian. That is, the Laplace estimator is essentially nonlinear [7, 6]. Additionally, the structure of the Laplace pdfs naturally facilitates the development of objective functions with L_1 costs, allowing for L_1 controller design using the tools developed for the Laplace estimator [5, 22, 6].

The scalar Laplace pdf with zero mean and variance $2\alpha^2$ has the form

$$f_L(x) = \frac{1}{2\alpha} e^{-\frac{1}{\alpha}|x|}. \tag{1.1}$$

Contrast this with the pdfs for the Cauchy distribution, $f_C(x)$, with zero median and Gaussian distribution, $f_G(x)$, with zero mean and variance σ^2,

$$\begin{aligned} f_C(x) &= \frac{\beta/\pi}{\beta^2 + x^2}, \\ f_G(x) &= \frac{1}{\sqrt{2\pi\sigma^2}} e^{-\frac{x^2}{2\sigma^2}}. \end{aligned} \tag{1.2}$$

Figure 1 shows plots of the Cauchy, Laplace, and Gaussian pdfs and observes the heaviness of the Cauchy tails compared to those of the other two. While the Laplace tails still overbound those of the Gaussian, we can see that they do decay exponentially and are much lighter than those of the Cauchy pdf.

The Gaussian, Laplace and Cauchy estimators can be distinguished by their a posteriori conditional pdfs (cdpfs) of the state given a measurements sequence. The

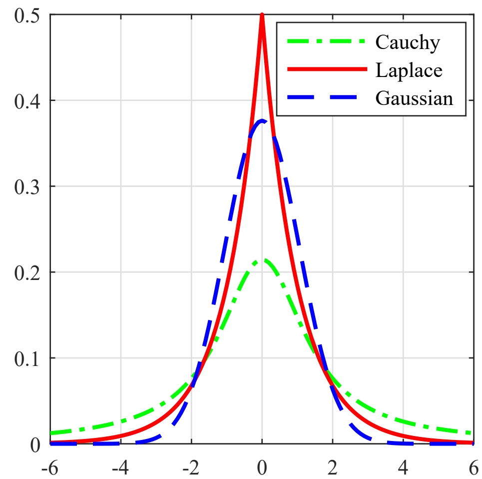

FIG. 1. *Comparison of pdfs.*

Kalman filter's a posteriori cpdf is Gaussian and is therefore both symmetric and unimodal. In contrast, the Cauchy a posteriori cpdf is neither symmetric nor unimodal. Finally, the Laplace a posteriori cpdf is not symmetric but is unimodal. Like the Kalman filter and Cauchy estimator, the Laplace conditional mean state estimate is the exact minimum-variance estimator for a linear system with additive Laplace noise, and is not an approximation. In addition, like the Cauchy, the Laplace conditional variance was shown to be a function of the measurements as well as the noise parameters. In contrast, the Kalman filter variance can be computed a priori. One can see the consequences of this when the Kalman filter processes Cauchy noise [11]. While the Laplace pdfs do not model volatility as well as Cauchy distributions, the Laplace estimator still handles outliers well.

In this study, we present the vector-state form of a Laplace estimator, which is an extension of the scalar case [7]. In section 2, we formulate the discrete-time, time-varying, linear vector-state system with additive scalar Laplace noises and define the estimation problem. In section 3, we derive the unnormalized conditional pdfs (ucpdfs) of the state given the first measurement and time propagation steps to deduce the general recursive form. It is shown that the cpdf is composed of signs and absolute values of affine functions of the state. In section 3.3, a basis composed of signs of affine functions is constructed which simplifies the representation of factors in the cpdf. The integral formula of [12] that is central to the derivation of the Laplace estimator is generalized to allow for products of sign functions with affine arguments to accommodate the new basis functions in section 3.4. After we prove the recursion of the general form of the conditional density functions of the state given a measurement sequence by induction in section 4, we derive the closed-form equations for the mean and variance using characteristic functions in section 5. In section 6, we present a numerical simulation for the $\mathbb{R}^2$ case as an initial demonstration of the estimation algorithm and comment on some computational aspects. Finally, we offer some concluding remarks in section 7.

2. Problem statement. Let the linear discrete-time system with state $\tilde{\boldsymbol{x}}_k \in \mathbb{R}^n$, scalar measurement $z_k \in \mathbb{R}$, independent scalar measurement noise v_k, and independent scalar process noise w_k be defined as

$$\begin{aligned}\tilde{\boldsymbol{x}}_{k+1} &= \Phi\tilde{\boldsymbol{x}}_k + \Gamma w_k,\\ \tilde{z}_k &= H\tilde{\boldsymbol{x}}_k + v_k\end{aligned} \tag{2.1}$$

with known $\Phi \in \mathbb{R}^{n\times n}$, $\Gamma \in \mathbb{R}^{n\times 1}$, and $H \in \mathbb{R}^{1\times n}$. Also let $\tilde{\boldsymbol{x}}_1, w_k$, and v_k all be Laplace distributed as

$$f_{\tilde{X}_1}(\tilde{\boldsymbol{x}}_1) = \prod_{i=1}^{n} \frac{1}{2\alpha} e^{-\frac{1}{\alpha}|\tilde{x}_i - \bar{x}_i|} = \prod_{i=1}^{n} \frac{1}{2\alpha} e^{-\frac{1}{\alpha}|-\bar{x}_i + E_i\tilde{\boldsymbol{x}}_1|} \triangleq \frac{1}{(2\alpha)^n}\bar{f}_{\tilde{X}_1}(\tilde{\boldsymbol{x}}_1), \tag{2.2}$$

$$f_W(w_k) = \frac{1}{2\beta} e^{-\frac{1}{\beta}|w_k|} \triangleq \frac{1}{2\beta}\bar{f}_W(w_k), \tag{2.3}$$

$$f_V(v_k) = \frac{1}{2\gamma} e^{-\frac{1}{\gamma}|v_k|} \triangleq \frac{1}{2\gamma}\bar{f}_V(v_k), \tag{2.4}$$

where the elements of $\tilde{\boldsymbol{x}}_1$ are mutually independent, and $E_i \in \mathbb{R}^{1\times n}$ have elements 1 at i and 0 elsewhere. All of the system and pdf parameters are time-varying, but an explicit dependence of k is suppressed for notational simplicity.

For convenience, we decompose the system state into a deterministic part $\bar{\boldsymbol{x}}_k$ and a stochastic part $\boldsymbol{x}_k$, so that

$$\tilde{\boldsymbol{x}}_k = \bar{\boldsymbol{x}}_k + \boldsymbol{x}_k, \tag{2.5}$$

where the deterministic state system is

$$\bar{\boldsymbol{x}}_{k+1} = \Phi\bar{\boldsymbol{x}}_k, \qquad \bar{z}_k = H\bar{\boldsymbol{x}}_k, \tag{2.6}$$

with initial conditions $\bar{\boldsymbol{x}}_1 = \begin{bmatrix} \bar{x}_1 & \bar{x}_2 & \cdots & \bar{x}_n \end{bmatrix}^T$, and the stochastic state system is

$$\boldsymbol{x}_{k+1} = \Phi\boldsymbol{x}_k + \Gamma w_k, \qquad z_k = H\boldsymbol{x}_k + v_k, \tag{2.7}$$

with initial conditions

$$f_{X_1}(\boldsymbol{x}_1) = \prod_{i=1}^{n} \frac{1}{2\alpha} e^{-\frac{1}{\alpha}|E_i\boldsymbol{x}_1|} \triangleq \frac{1}{(2\alpha)^n}\bar{f}_{X_1}(\boldsymbol{x}_1). \tag{2.8}$$

For the remainder of the derivation, we will only consider the stochastic part of the state, $\boldsymbol{x}_k$ (2.7).

In what follows, we will use the following convention for the sign function, $\operatorname{sgn}(\xi) : \mathbb{R} \to \mathbb{R}$ such that

$$\operatorname{sgn}(\xi) = \begin{cases} -1, & \xi \le 0, \\ +1, & \xi > 0, \end{cases} \tag{2.9}$$

where, for $\psi \in \mathbb{R}$ and $\theta, \boldsymbol{x} \in \mathbb{R}^n$,

$$\xi = \psi + \theta\boldsymbol{x}, \tag{2.10}$$

and θ is a row vector. We will limit our presentation to causal dynamical systems, which have unique solutions, and invertible Φ, thereby eliminating dead-beat systems.

The goal of this paper is to develop the conditional density function (cpdf) of the state $\boldsymbol{X}_k$, given a measurement sequence

$$\boldsymbol{Y}_k = \{Z_1, Z_2, \ldots, Z_k\}, \tag{2.11}$$

in an analytic form for the Laplace system described in (2.7), from which we will determine the mean and variance for the minimum-variance estimator. The sequence

$$\boldsymbol{y}_k = \{z_1, z_2, \ldots, z_k\} \tag{2.12}$$

is a realization of (2.11). To streamline the derivation and improve legibility, we will use the unnormalized pdfs $\bar{f}_W, \bar{f}_V$, and $\bar{f}_{\boldsymbol{X}_1}$ in (2.3), (2.4), and (2.8) to construct the cpdf. This avoids having to keep account of the normalizing factor, which can be computed as necessary, e.g., when determining the mean and variance.

3. Laplace cpdf. To determine the recursive form of the cpdf, we examine the first measurement update and time propagation. We begin with the initial pdf, $\bar{f}_{\boldsymbol{X}_1}$, and compute the a posteriori cpdf of $\boldsymbol{X}_1$, conditioned on a measurement z_1. This is followed by a time propagation to $\boldsymbol{X}_2$. Continuing in this way, we can deduce and then prove the recursive structure of the a priori and a posteriori cpdfs.

We explicitly compute the first measurement update and time propagation steps for the two-dimensional case to motivate the general structure of the ucpdf as well as the recursive algorithm to generate successive a posteriori and a priori ucpdfs at any step k for the general n-dimensional case.

For the initial two-dimensional pdf, we use (2.8) where $n = 2$, and let the elements of initial condition be described by independent Laplace distributions with means 0 and with spread parameter α so that

$$\bar{f}_{\boldsymbol{X}_1}(\boldsymbol{x}_1) = \exp\left(-\frac{1}{\alpha}\left|E_1\boldsymbol{x}_1\right| - \frac{1}{\alpha}\left|E_2\boldsymbol{x}_1\right|\right), \tag{3.1}$$

where

$$E_1 = \begin{bmatrix} 1 & 0 \end{bmatrix}, \quad E_2 = \begin{bmatrix} 0 & 1 \end{bmatrix}. \tag{3.2}$$

3.1. Update at $\boldsymbol{k = 1}$. Let the measurement at $k = 1$ be z_1 so that, using (2.4) and (2.7), the density of Z_1 conditioned on $\boldsymbol{X}_1$ is

$$\bar{f}_{Z_1|\boldsymbol{X}_1}(z_1|\boldsymbol{x}_1) = \bar{f}_V\left(z_1 - H\boldsymbol{x}_1\right) = \exp\left(-\frac{1}{\gamma}\left|z_1 - H\boldsymbol{x}_1\right|\right). \tag{3.3}$$

The pdf of $\boldsymbol{X}_1$ conditioned on Z_1 is given by Bayes' theorem,

$$f_{\boldsymbol{X}_1|\boldsymbol{Y}_1}(\boldsymbol{x}_1|\boldsymbol{y}_1) = \frac{f_{\boldsymbol{Y}_1|\boldsymbol{X}_1}(\boldsymbol{y}_1|\boldsymbol{x}_1)f_{\boldsymbol{X}_1}(\boldsymbol{x}_1)}{f_{\boldsymbol{Y}_1}(\boldsymbol{y}_1)}, \tag{3.4}$$

where $\boldsymbol{y}_1 = \{z_1\}$. As mentioned before, we will derive the ucpdf going forward, or

$$\bar{f}_{\boldsymbol{X}_1|\boldsymbol{Y}_1}(\boldsymbol{x}_1|\boldsymbol{y}_1) = \bar{f}_{\boldsymbol{Y}_1|\boldsymbol{X}_1}(\boldsymbol{y}_1|\boldsymbol{x}_1)\bar{f}_{\boldsymbol{X}_1}(\boldsymbol{x}_1) = \bar{f}_{Z_1|\boldsymbol{X}_1}(z_1|\boldsymbol{x}_1)\bar{f}_{\boldsymbol{X}_1}(\boldsymbol{x}_1). \tag{3.5}$$

Using (3.1) and (3.3), this becomes

$$\begin{aligned} \bar{f}_{\boldsymbol{X}_1|\boldsymbol{Y}_1} &= \bar{f}_{\boldsymbol{X}_1}(\boldsymbol{x}_1)\bar{f}_V(z_1 - H\boldsymbol{x}_1) \\ &= \exp\left(-\frac{1}{\alpha}\left|E_1\boldsymbol{x}_1\right| - \frac{1}{\alpha}\left|E_2\boldsymbol{x}_1\right| - \frac{1}{\gamma}\left|z_1 - H\boldsymbol{x}_1\right|\right). \end{aligned} \tag{3.6}$$

Figure 2 shows $\bar{f}_{\boldsymbol{X}_1|\boldsymbol{Y}_1}$ for $H = \begin{bmatrix} 1 & 0.5 \end{bmatrix}$ with noise parameters $\alpha = 0.3$ and $\gamma = 0.1$. The initial deterministic states were set to $\bar{\boldsymbol{x}}_1 = \begin{bmatrix} 0.2 \\ -1.3 \end{bmatrix}$. Notice the asymmetry and kink on the left side, which is the peak of $\bar{f}_V(z_1 - H\boldsymbol{x}_1)$.

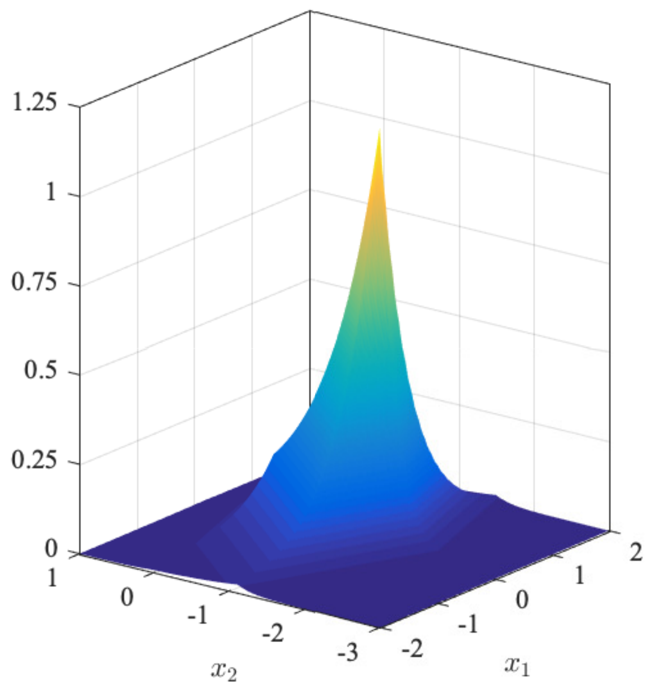

FIG. 2. $\bar{f}_{X_1|Y_1}$: *a posteriori ucpdf at* $k = 1$.

3.2. Propagation from $k = 1$ to $k = 2$. To determine the ucpdf $\bar{f}_{\boldsymbol{X}_2|\boldsymbol{Y}_1}(\boldsymbol{x}_2|\boldsymbol{y}_1)$, we first construct the joint density $\bar{f}_{\boldsymbol{X}_2,W|\boldsymbol{Y}_1}$. Since W is independent of $\boldsymbol{X}_1$ and $\boldsymbol{Y}_1$,

$$\bar{f}_{\boldsymbol{X}_1,W|\boldsymbol{Y}_1} = \bar{f}_{\boldsymbol{X}_1|\boldsymbol{Y}_1}\bar{f}_W, \tag{3.7}$$

where $\bar{f}_W$ is given in (2.3). Next, we express $\boldsymbol{x}_1$ in terms of $\boldsymbol{x}_2$ and w_1 by using (2.7) and then integrate with respect to w_1. For the initial conditions, each term in the exponent becomes

$$\begin{aligned} -\frac{1}{\alpha}\left|E_i\boldsymbol{x}_1\right| &= -\frac{1}{\alpha}\left|E_i\left(\Phi^{-1}\boldsymbol{x}_2\right) - E_i\Phi^{-1}\Gamma w_1\right| \\ &= -\frac{\left|E_i\Phi^{-1}\Gamma\right|}{\alpha}\left|\frac{E_i\Phi^{-1}\boldsymbol{x}_2}{E_i\Phi^{-1}\Gamma} - w_1\right|, \end{aligned} \tag{3.8}$$

where $i = 1, 2$, while the exponent for the measurement becomes

$$\begin{aligned} -\frac{1}{\gamma}\left|z_1 - H\boldsymbol{x}_1\right| &= -\frac{1}{\alpha}\left|-\bar{z}_1 + H\left(\Phi^{-1}\boldsymbol{x}_2\right) - H\Phi^{-1}\Gamma w_1\right| \\ &= -\frac{\left|H\Phi^{-1}\Gamma\right|}{\gamma}\left|\frac{-z_1}{H\Phi^{-1}\Gamma} + \frac{H\Phi^{-1}\boldsymbol{x}_2}{H\Phi^{-1}\Gamma} - w_1\right|. \end{aligned} \tag{3.9}$$

Using (2.3) and (3.6),

$$\begin{aligned}(3.10)\quad &\bar{f}_{X_2|Y_1}(\boldsymbol{x}_2|\boldsymbol{y}_1)\\ &= \left|\Phi^{-1}\right| \int_{-\infty}^{\infty} \exp\left(-\frac{\left|E_1\Phi^{-1}\Gamma\right|}{\alpha}\left|\frac{E_1\Phi^{-1}\boldsymbol{x}_2}{E_1\Phi^{-1}\Gamma} - w_1\right| - \frac{\left|E_2\Phi^{-1}\Gamma\right|}{\alpha}\left|\frac{E_2\Phi^{-1}\boldsymbol{x}_2}{E_2\Phi^{-1}\Gamma} - w_1\right|\right.\\ &\qquad\left. - \frac{\left|H\Phi^{-1}\Gamma\right|}{\gamma}\left|\frac{-z_1}{H\Phi^{-1}\Gamma} + \frac{H\Phi^{-1}\boldsymbol{x}_2}{H\Phi^{-1}\Gamma} - w_1\right| - \frac{1}{\beta}\left|w_1\right|\right) dw_1,\end{aligned}$$

where $\left|\Phi^{-1}\right| \triangleq \det\left(\Phi^{-1}\right)$ and it is assumed that $E_1\Phi^{-1}\Gamma \neq 0$, $E_2\Phi^{-1}\Gamma \neq 0$, and $H\Phi^{-1}\Gamma \neq 0$. Using the integral formula (A.6), which generalizes the closed-form integral in Appendix B of [12], and defining integration parameters $\bar{\rho}_i^{2|1}$ and $\bar{\xi}_i^{2|1}$ as

$$(3.11)\quad \begin{aligned} \bar{\rho}_1^{2|1} &= \frac{\left|E_1\Phi^{-1}\Gamma\right|}{\gamma}, & \bar{\xi}_1^{2|1} &= \frac{E_1\Phi^{-1}\boldsymbol{x}_2}{E_1\Phi^{-1}\Gamma} \triangleq \bar{\psi}_1^{2|1} + \bar{\theta}_1^{2|1}\boldsymbol{x}_2,\\ \bar{\rho}_2^{2|1} &= \frac{\left|E_2\Phi^{-1}\Gamma\right|}{\gamma}, & \bar{\xi}_2^{2|1} &= \frac{E_2\Phi^{-1}\boldsymbol{x}_2}{E_2\Phi^{-1}\Gamma} \triangleq \bar{\psi}_2^{2|1} + \bar{\theta}_2^{2|1}\boldsymbol{x}_2,\\ \bar{\rho}_3^{2|1} &= \frac{\left|H\Phi^{-1}\Gamma\right|}{\gamma}, & \bar{\xi}_3^{2|1} &= \frac{-z_1}{H\Phi^{-1}\Gamma} + \frac{H\Phi^{-1}\boldsymbol{x}_2}{H\Phi^{-1}\Gamma} \triangleq \bar{\psi}_3^{2|1} + \bar{\theta}_3^{2|1}\boldsymbol{x}_2,\\ \bar{\rho}_4^{2|1} &= \frac{1}{\beta}, & \bar{\xi}_4^{2|1} &= 0 \triangleq \bar{\psi}_4^{2|1} + \bar{\theta}_4^{2|1}\boldsymbol{x}_2,\end{aligned}$$

the solution to (3.10) is

$$(3.12)\quad \bar{f}_{X_2|Y_1}(\boldsymbol{x}_2|\boldsymbol{y}_1) = \sum_{j=1}^{4} g_j^{2|1}\exp\left(-\sum_{\substack{l=1\\l\neq j}}^{4}\rho_l^{2|1}\left|\xi_l^{2|1} - \xi_j^{2|1}\right|\right) \triangleq \sum_{j=1}^{4} g_j^{2|1}\epsilon_j^{2|1},$$

where

$$\begin{aligned}(3.13)\quad g_j^{2|1}(\boldsymbol{x}_2) &= \frac{\left|\Phi^{-1}\right|}{\bar{\rho}_j^{2|1} + \sum\limits_{\substack{l=1\\l\neq j}}^{4}\bar{\rho}_l^{2|1}\operatorname{sgn}\left(\bar{\xi}_l^{2|1} - \bar{\xi}_j^{2|1}\right)} - \frac{\left|\Phi^{-1}\right|}{-\bar{\rho}_j^{2|1} + \sum\limits_{\substack{l=1\\l\neq j}}^{4}\rho_l^{2|1}\operatorname{sgn}\left(\bar{\xi}_l^{2|1} - \bar{\xi}_j^{2|1}\right)}\\ &\triangleq \frac{\left|\Phi^{-1}\right|}{\bar{\rho}_j^{2|1} + \sum\limits_{\substack{l=1\\l\neq j}}^{4}\rho_l^{2|1}\operatorname{sgn}\left(\psi_{jl}^{2|1} + \theta_{jl}^{2|1}\boldsymbol{x}_2\right)} - \frac{\left|\Phi^{-1}\right|}{-\bar{\rho}_j^{2|1} + \sum\limits_{\substack{l=1\\l\neq j}}^{4}\rho_l^{2|1}\operatorname{sgn}\left(\psi_{jl}^{2|1} + \theta_{jl}^{2|1}\boldsymbol{x}_2\right)}\end{aligned}$$

and

$$(3.14)\quad \epsilon_j^{2|1}(\boldsymbol{x}_2) = \exp\left(-\sum_{\substack{l=1\\l\neq j}}^{4}\bar{\rho}_l^{2|1}\left|\bar{\xi}_l^{2|1} - \bar{\xi}_j^{2|1}\right|\right) \triangleq \exp\left(-\sum_{\substack{l=1\\l\neq j}}^{4}\bar{\rho}_l^{2|1}\left|\psi_{jl}^{2|1} + \theta_{jl}^{2|1}\boldsymbol{x}_2\right|\right).$$

Note that we've converted the arguments of the sign functions into standard form, where $\psi_{jl}^{2|1} = \bar{\psi}_l^{2|1} - \bar{\psi}_j^{2|1}$ and $\theta_{jl}^{2|1} = \bar{\theta}_l^{2|1} - \bar{\theta}_j^{2|1}$. In addition, $\psi_{jl}^{2|1} + \theta_{jl}^{2|1}\boldsymbol{x}$ is affine and, where it is zero, defines a hyperplane (which is a line in $\mathbb{R}^2$). In the next subsection, it is shown how the g_j function in (3.13) can be simplified by determining a basis constructed from these hyperplanes.

3.3. Simplify g after propagation. The form of the coefficient function g_j in (3.13) is not suitable for recursion, because it produces a complicated, nested fraction which quickly becomes intractable. Furthermore, it is impractical to combine any terms in (3.12), which share the same argument of the exponential while dealing with such an unwieldy coefficient function. However, we can transform g_j into a sum of sign basis functions, which solves both of these issues, using the following theorem.

THEOREM 3.1. *Let $\mathcal{A}$ be a hyperplane arrangement of m affine hyperplanes $A_1, \dots, A_m$ in $\mathbb{R}^n$, where $A_i = \{\boldsymbol{x} | \psi_i + \theta_i \boldsymbol{x} = 0\}$, $\theta_i^T, \boldsymbol{x} \in \mathbb{R}^n, \psi_i \in \mathbb{R}$. Let $g : \mathbb{R}^n \to \mathbb{R}$ be a function of $sgn(\psi_i + \theta_i \boldsymbol{x})$, which is thus constant on the n-dimensional faces of $\mathcal{A}$. Then, g can be expressed as*

$$g = \sum_{j=0}^{P} \rho_j \prod_{l \in \sigma_j} sgn(\psi_l + \theta_l \boldsymbol{x}), \tag{3.15}$$

where $\sigma_j \in \sigma$, which is the set of all subsets of $\{1, \dots, m\}$ with cardinality n or less, and $P = \sum_{k=0}^{n} \binom{m}{k}$. For $\sigma_j = \emptyset$, the product in (3.15) *reduces to* 1 *and the corresponding term is constant.*

Proof. The proof of this theorem is presented in [4]. ☐

COROLLARY 3.2. *Let S be defined as*

$$S \triangleq \begin{bmatrix} 1 & s_1 & \cdots & s_m & s_1 s_2 & \cdots & s_{m-1} s_m & \cdots & s_{m-n+1} \cdots s_m \end{bmatrix}, \tag{3.16}$$

where $s_i = sgn(\psi_i + \theta_i \boldsymbol{x})$. Then S is a basis for g.

Proof. This is clear from the representation of g in (3.15). ☐

Theorem 3.1 has a profound effect on the general n-dimensional Laplace estimator. Not only does it make more obvious how we can preserve the structure of the ucpdf under propagation, it provides a straightforward framework for combining terms simply by adding coefficients.

To illustrate the application of Theorem 3.1, we show the form of $g_1^{2|1}(\boldsymbol{x}_2)$ for $\boldsymbol{x} \in \mathbb{R}^2$ after it has been transformed from the fractional form in (3.13) to a sum of basis functions. The algorithm to determine the coefficients is described in Appendix B. $g_1(\boldsymbol{x}_2)$ then assumes the form

$$\begin{aligned} g_1^{2|1}(\boldsymbol{x}_2) = \rho_{10}^{2|1} &+ \rho_{11}^{2|1} \operatorname{sgn}\left(\psi_{11}^{2|1} + \theta_{11}^{2|1} \boldsymbol{x}_2\right) \\ &+ \rho_{12}^{2|1} \operatorname{sgn}\left(\psi_{12}^{2|1} + \theta_{12}^{2|1} \boldsymbol{x}_2\right) + \rho_{13}^{2|1} \operatorname{sgn}\left(\psi_{13}^{2|1} + \theta_{13}^{2|1} \boldsymbol{x}_2\right) \\ &+ \rho_{14}^{2|1} \operatorname{sgn}\left(\psi_{11}^{2|1} + \theta_{11}^{2|1} \boldsymbol{x}_2\right) \operatorname{sgn}\left(\psi_{12}^{2|1} + \theta_{12}^{2|1} \boldsymbol{x}_2\right) \\ &+ \rho_{15}^{2|1} \operatorname{sgn}\left(\psi_{11}^{2|1} + \theta_{11}^{2|1} \boldsymbol{x}_2\right) \operatorname{sgn}\left(\psi_{13}^{2|1} + \theta_{13}^{2|1} \boldsymbol{x}_2\right) \\ &+ \rho_{16}^{2|1} \operatorname{sgn}\left(\psi_{12}^{2|1} + \theta_{12}^{2|1} \boldsymbol{x}_2\right) \operatorname{sgn}\left(\psi_{13}^{2|1} + \theta_{13}^{2|1} \boldsymbol{x}_2\right) \\ = \rho_{10}^{2|1} &+ \sum_{j=1}^{6} \rho_{1j}^{2|1} \prod_{l \in \sigma_j} \operatorname{sgn}\left(\psi_{1i}^{2|1} + \theta_{1i}^{2|1} \boldsymbol{x}_2\right), \end{aligned} \tag{3.17}$$

where

$$\sigma_j = \{\{1\}, \{2\}, \{3\}, \{1,2\}, \{1,3\}, \{2,3\}\}, \tag{3.18}$$

and the basis function is a constant (i.e., 1), a single sign function, or product of two sign functions. Note that the number of nonconstant terms is $\binom{3}{1} + \binom{3}{2} = 3 + 3 = 6$.

Figure 3 shows $\bar{f}_{X_2|Y_1}$ for system parameters

$$\Phi = \begin{bmatrix} 0.95 & 0.01 \\ -0.1 & 1 \end{bmatrix}, \qquad \Gamma = \begin{bmatrix} 0 \\ 1 \end{bmatrix}, \qquad H = \begin{bmatrix} 1 & 0.5 \end{bmatrix} \tag{3.19}$$

with initial conditions

$$\bar{\boldsymbol{x}}_1 = \begin{bmatrix} 0.2 \\ -1.3 \end{bmatrix}, \tag{3.20}$$

and noise parameters $\alpha = 0.3$, $\beta = 0.01$, and $\gamma = 0.1$. Note the smoothness (twice-differentiable; see section 5.2 of [12]) of the pdf after convolution with f_W compared to the sharp point of $\bar{f}_{X_1|Y_1}$ in Figure 2.

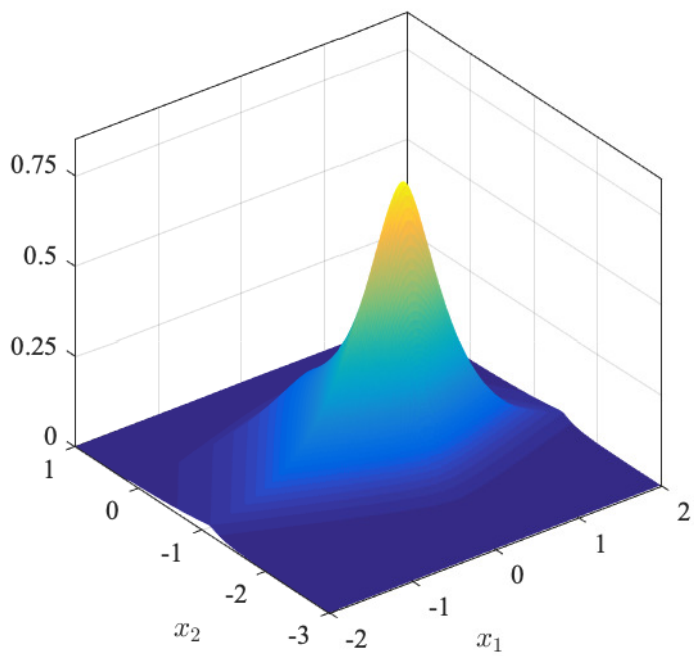

FIG. 3. $\bar{f}_{X_2|Y_1}$: *a priori ucpdf from $k = 1$ to $k = 2$.*

3.4. Generalized integral formula. The simplification of the coefficient function in (3.17) introduces a complication. The integral formula that we've been using to propagate $\bar{f}_{X_k|Y_k}$ was derived in [12] and is not valid when g is not a function of sums of signs. Therefore, we rederived the integral formula to account for the products of sign functions in Appendix A. In fact, Appendix A is valid for any function g constant on intervals of the real axis. The results in the relevant form in (A.6) are restated here for convenience. For some $M, P \in \mathbb{Z}^+$ and

$$g(w) = \rho_0 + \sum_{j=1}^{P} \rho_j \prod_{\ell \in \sigma_j} \operatorname{sgn}(\xi_\ell - w), \tag{3.21}$$

where σ_j is one of P unique subset of $\{1, \ldots, M\}$,

$$\int_{-\infty}^{\infty} g(w) \exp\left(-\sum_{\ell=1}^{M} \eta_i \left|\xi_\ell - w\right|\right) dw = \sum_{i=1}^{M} g_i(\xi_i) \exp\left(-\sum_{\ell=1}^{M} \rho_\ell \left|\xi_\ell - \xi_i\right|\right), \tag{3.22}$$

where

$$g_i(\xi_i) = \frac{g(\xi_i)^\dagger}{\eta_i + \sum\limits_{\substack{\ell=1\\ \ell\neq i}}^{M} \eta_\ell \operatorname{sgn}(\xi_\ell - \xi_i)} - \frac{g(\xi_i)}{-\eta_i + \sum\limits_{\substack{\ell=1\\ \ell\neq i}}^{M} \eta_\ell \operatorname{sgn}(\xi_\ell - \xi_i)}, \tag{3.23}$$

and the $\dagger$ on the left term of (3.23) indicates a special case where, for

$$g^\dagger(\xi_i) = \rho_0 + \sum_{j=1}^{P} \rho_j \prod_{\ell\in\sigma_j} \operatorname{sgn}(\xi_\ell - \xi_i), \tag{3.24}$$

all instances of $\operatorname{sgn}(\xi_\ell - \xi_i) = 1$ when $\ell = i$. In contrast, for $g(\xi_i)$ on the right term of (3.23), $\operatorname{sgn}(\xi_\ell - \xi_i) = -1$ when $\ell = i$. Since this is consistent with the original definition of $\operatorname{sgn}(\xi)$ in (2.9), it is not considered a special case. The denominators of (3.23) apply these different definitions for $\operatorname{sgn}(\xi_\ell - \xi_i)$ when $\ell = i$, and the substitutions have been made explicitly, resulting in the η_i and $-\eta_i$ terms. This integral formula allows for the propagation in $\mathbb{R}^n$ as well as calculation of the moments in section 5.

4. General form of ucpdf: Proof by induction for $\mathbb{R}^n$.

We now present the recursive algorithm for determining the a posteriori and a priori ucpdfs at step $k+1|k$ by undergoing a measurement update from step $k|k-1$ to $k|k$, followed by a propagation step requiring a convolution integral. Finally, we organize these results into the standard structure.

4.1. Induction hypothesis in $\mathbb{R}^n$.

Suppose we are given the a priori ucpdf at $k|k-1$

$$\bar{f}_{X_k|Y_{k-1}} = \sum_{i=1}^{N_i^{k|k-1}} g_i^{k|k-1} \epsilon_i^{k|k-1}, \tag{4.1}$$

where $g_i^{k|k-1}$ is manipulated into the form in (3.15) as

$$g_i^{k|k-1} = \rho_{i0} + \sum_{j=1}^{P_i^{k|k-1}} \rho_{ij}^{k|k-1} \prod_{l\in\sigma_{ij}} \operatorname{sgn}\left(\xi_{il}^{k|k-1}\right), \tag{4.2}$$

and

$$\epsilon_i^{k|k-1} = \exp\left(-\sum_{j=1}^{M_i^{k|k-1}} \eta_{ij}^{k|k-1} \left|\xi_{ij}^{k|k-1}\right|\right). \tag{4.3}$$

The affine function of $\boldsymbol{x}_k$ is

$$\xi_{ij}^{k|k-1} = \psi_{ij}^{k|k-1} + \theta_{ij}^{k|k-1} \boldsymbol{x}_k, \tag{4.4}$$

where $N_i^{k|k-1}$ is the number of terms, $M_i^{k|k-1}$ is the number of elements of term i, $P_i^{k|k-1}$ is the number of terms in $g_i^{k|k-1}$, and σ_{ij} is the set of indices of sign functions associated with term j of $g_i^{k|k-1}$ at step $k|k-1$.

4.2. Measurement update from $k|k-1$ to $k|k$. By construction, we know that the ucpdf at 2|1 from section 3 has the form shown in (4.1). Therefore, we assume $\bar{f}_{X_k|Y_{k-1}}$ in (4.1) and show that $\bar{f}_{X_{k+1},Y_k}$ has the same structure.

The measurement update step involves constructing the joint density from the a priori ucpdf (4.1) and

$$\bar{f}_{Z_k|\boldsymbol{X}_k} = \bar{f}_V(z_k - H\boldsymbol{x}_k) = \exp\left(-\frac{1}{\gamma}\left|z_k - H\boldsymbol{x}_k\right|\right). \tag{4.5}$$

Since V is independent measurement noise, the ucpdf for $\boldsymbol{X}_k$ given $\boldsymbol{Y}_k$ is obtained by Bayes' theorem using (4.5) and (4.1) and effectively contributes an additional element to the exponential in (4.1) so that

$$\bar{f}_{\boldsymbol{X}_k|\boldsymbol{Y}_k} = \sum_{i=1}^{N_i^{k|k-1}} g_i^{k|k}\epsilon_i^{k|k}, \tag{4.6}$$

where $g_i^{k|k} = g_i^{k|k-1}$ and

$$\begin{aligned}\epsilon_i^{k|k} &= \exp\left(-\sum_{j=1}^{M_i^{k|k-1}} \eta_{ij}^{k|k-1}\left|\xi_{ij}^{k|k-1}\right| - \frac{1}{\gamma}\left|-z_k + H\boldsymbol{x}_k\right|\right)\\ &= \exp\left(-\sum_{j=1}^{M_i^{k|k-1}+1} \eta_{ij}^{k|k-1}\left|\xi_{ij}^{k|k-1}\right|\right),\end{aligned} \tag{4.7}$$

with

$$\xi_{ij}^{k|k-1} = \psi_{ij}^{k|k-1} + \theta_{ij}^{k|k-1}\boldsymbol{x}_k. \tag{4.8}$$

This gives us the a posteriori ucpdf at $k|k$, with the additional parameters

$$\rho_{i,M_i^{k|k-1}+1}^{k|k-1} = \frac{1}{\gamma}, \qquad \psi_{i,M_i^{k|k-1}+1}^{k|k-1} = -z_k, \qquad \theta_{i,M_i^{k|k-1}+1}^{k|k-1} = H \tag{4.9}$$

4.3. Propagation from $k|k$ to $k+1|k$. The propagation of the ucpdf involves constructing the joint density function of $\bar{f}_{\boldsymbol{X}_k|\boldsymbol{Y}_k}$ and f_W and integrating with respect to w_k. Given (4.6), the a priori ucpdf at $k+1$ is

$$\bar{f}_{\boldsymbol{X}_{k+1}|\boldsymbol{Y}_k}(\boldsymbol{x}_{k+1}|\boldsymbol{y}_k) = \int_{-\infty}^{\infty} \bar{f}_{\boldsymbol{X}_k|\boldsymbol{Y}_k}(\boldsymbol{x}_k|\boldsymbol{y}_k)\bar{f}_W(w_k)\,dw_k. \tag{4.10}$$

In order to perform this integral, we write $\boldsymbol{x}_k$ in terms of $(\boldsymbol{x}_{k+1}, w_k)$ using the dynamical equation in (2.7) and the derived density formula in [23, p. 51] to get

$$\begin{aligned}&\begin{bmatrix}\boldsymbol{x}_{k+1}\\ w_k\end{bmatrix} = \begin{bmatrix}\Phi & \Gamma\\ 0 & I\end{bmatrix}\begin{bmatrix}\boldsymbol{x}_k\\ w_k\end{bmatrix} \triangleq A\begin{bmatrix}\boldsymbol{x}_k\\ w_k\end{bmatrix}\\ &\implies \begin{bmatrix}\boldsymbol{x}_k\\ w_k\end{bmatrix} = \begin{bmatrix}\Phi^{-1} & -\Phi^{-1}\Gamma\\ 0 & 1\end{bmatrix}\begin{bmatrix}\boldsymbol{x}_{k+1}\\ w_k\end{bmatrix} \triangleq A^{-1}\begin{bmatrix}\boldsymbol{x}_{k+1}\\ w_k\end{bmatrix}.\end{aligned} \tag{4.11}$$

We then integrate with respect to w_k,

$$\begin{aligned}&\bar{f}_{X_{k+1}|Y_k}(\boldsymbol{x}_{k+1}|\boldsymbol{y}_k)\\ &\qquad = \left|\Phi^{-1}\right|\int_{-\infty}^{\infty} \bar{f}_{X_k|Y_k}\left(\Phi^{-1}\boldsymbol{x}_{k+1} - \Phi^{-1}\Gamma w_k|\boldsymbol{y}_k\right)\bar{f}_W(w_k)\,dw_k,\end{aligned} \tag{4.12}$$

where $\left|\Phi^{-1}\right| = \det\left(\Phi^{-1}\right) = \det\left(A^{-1}\right)$. Since f_W is an exponential of absolute value of w_k, we can rewrite the integrand into the same form as the integral formula in (3.22). Therefore, each term of $\bar{f}_{\boldsymbol{X}_{k+1}|\boldsymbol{Y}_k}$ becomes

$$\bar{f}^i_{\boldsymbol{X}_{k+1}|\boldsymbol{Y}_k}(\boldsymbol{x}_{k+1}|\boldsymbol{y}_k) = \int_{-\infty}^{\infty} \tilde{g}_i^{k|k}(\boldsymbol{x}_{k+1}, w_k)\tilde{\epsilon}_i^{k|k}(\boldsymbol{x}_{k+1}, w_k)\, dw_k, \tag{4.13}$$

where

$$\begin{aligned}
\tilde{g}_i^{k|k}(\boldsymbol{x}_{k+1}, w_k) &= \tilde{\rho}_{i0}^{k|k} + \sum_{j=1}^{P_i^{k-1|k}} \tilde{\rho}_{ij}^{k|k} \prod_{l\in\sigma_{ij}} \operatorname{sgn}\left(\tilde{\xi}_{il}^{k|k}(\boldsymbol{x}_{k+1}) - w_k\right),\\
\tilde{\epsilon}_i(\boldsymbol{x}_{k+1,w_k}) &= \exp\left(-\sum_{j=1}^{M_i^{k|k-1}+2} \tilde{\eta}_{ij}^{k|k}\left|\tilde{\xi}_{ij}^{k|k}(\boldsymbol{x}_{k+1}) - w_k\right|\right),\\
\tilde{\rho}_{i0}^{k|k} &= \frac{|\Phi|^{-1}}{2\beta}\rho_{i0}^{k|k},\\
\tilde{\rho}_{ij}^{k|k} &= \frac{|\Phi|^{-1}}{2\beta}\rho_{ij}^{k|k}\prod_{l\in\sigma_j}\operatorname{sgn}\left(\theta_{il}^{k|k}\Phi^{-1}\Gamma\right),\\
\tilde{\eta}_{ij}^{k|k} &= \eta_{ij}^{k|k}\cdot\frac{1}{\left|\theta_{ij}^{k|k}\Phi^{-1}\Gamma\right|},\\
\tilde{\xi}_{ij}^{k|k} &= \frac{\psi_{ij}^{k|k}}{\theta_{ij}^{T}\Phi^{-1}\Gamma} + \frac{\theta_{ij}^{k|k}\Phi^{-1}}{\theta_{ij}^{k|k}\Phi^{-1}\Gamma}\boldsymbol{x}_{k+1} \triangleq \tilde{\psi}_{ij}^{k|k} + \tilde{\theta}_{ij}^{k|k}\boldsymbol{x}_{k+1}.
\end{aligned} \tag{4.14}$$

Each term is then integrated using the generalized integral formula (3.22) to get

$$\begin{aligned}
&\tilde{f}_{i,X_{k+1}|Y_k}(\boldsymbol{x}_{k+1}|\boldsymbol{y}_k)\\
&\quad= \sum_{j=1}^{M_i^{k|k-1}+2} \tilde{g}_{ijl}^{k+1|k}\exp\left(-\sum_{l=1}^{M_i^{k|k-1}+2}\tilde{\eta}_{il}^{k|k}\left|\tilde{\xi}_{il}^{k|k} - \tilde{\xi}_{ij}^{k|k}\right|\right)\\
&\quad= \sum_{j=1}^{M_i^{k|k-1}+2} \tilde{g}_{ijl}^{k+1|k}\exp\left[-\sum_{l=1}^{M_i^{k|k-1}+2}\tilde{\eta}_{il}^{k|k}\left|\left(\tilde{\psi}_{il}^{k|k} - \tilde{\psi}_{ij}^{k|k}\right) + \left(\tilde{\theta}_{il}^{k|k} - \tilde{\theta}_{ij}^{k|k}\right)\boldsymbol{x}_{k+1}\right|\right]\\
&\quad\triangleq \sum_{j=1}^{M_i^{k|k-1}+2} \tilde{g}_{ijl}^{k+1|k}\exp\left(-\sum_{l=1}^{M_i^{k|k-1}+2}\tilde{\eta}_{il}^{k|k}\left|\tilde{\psi}_{ijl}^{k+1|k} + \tilde{\theta}_{ijl}^{k|k}\boldsymbol{x}_{k+1}\right|\right)\\
&\quad= \sum_{j=1}^{M_i^{k|k-1}+2} \tilde{g}_{ijl}^{k+1|k}\exp\left(-\sum_{l=1}^{M_i^{k|k-1}+2}\tilde{\eta}_{il}^{k|k}\left|\tilde{\xi}_{ijl}^{k+1|k}\right|\right),
\end{aligned} \tag{4.15}$$

where

$$\tilde{g}_{ijl}^{k+1|k} = \frac{\tilde{g}_i^{k|k}\left(\tilde{\xi}_{ij}^{k|k}\right)^{\dagger}}{\tilde{\eta}_{ij}^{k|k} + \sum_{\substack{l=1\\l\neq j}}^{M_i^{k-1|k}-2} \tilde{\eta}_{il}^{k|k}\operatorname{sgn}\left(\tilde{\xi}_{ijl}^{k+1|k}\right)} - \frac{\tilde{g}_i^{k|k}\left(\tilde{\xi}_{ij}^{k|k}\right)}{-\tilde{\eta}_{ij}^{k|k} + \sum_{\substack{l=1\\l\neq j}}^{M_i^{k-1|k}-2} \tilde{\eta}_{il}^{k|k}\operatorname{sgn}\left(\tilde{\xi}_{ijl}^{k+1|k}\right)} \tag{4.16}$$

and the $\dagger$ indicates that every instance of $\operatorname{sgn}\left(\tilde{\xi}_{il}^{k|k} - \tilde{\xi}_{ij}^{k|k}\right) = 1$ when $l = j$. Note that each new argument has the form

$$\begin{aligned} \tilde{\eta}_{ijl}^{k+1|k} &= \tilde{\eta}_{ij}^{k|k}, \\ \tilde{\xi}_{ijl}^{k+1|k} &= \tilde{\xi}_{il}^{k|k} - \tilde{\xi}_{ij}^{k|k} = \left(\tilde{\psi}_{il}^{k|k} - \tilde{\psi}_{ij}^{k|k}\right) + \left(\tilde{\theta}_{il}^{k|k} - \tilde{\theta}_{ij}^{k|k}\right)\boldsymbol{x}_{k+1} \\ &\triangleq \tilde{\psi}_{ijl}^{k+1|k} + \tilde{\theta}_{ijl}^{k+1|k}\boldsymbol{x}_{k+1}. \end{aligned} \tag{4.17}$$

In the next subsections, we will reindex the triple indexing as well as the number of terms to prepare for the next measurement update.

4.4. Simplify coefficient function and reindex terms. The coefficient term in (4.16) is transformed from its fraction form into the basis form of (4.2) using the procedures outlined in Appendix B so that

$$\tilde{g}_{ijl}^{k+1|k} = \tilde{\rho}_{ij0}^{k+1|k} + \sum_{p=1}^{P_{ijl}^{k+1|k}} \tilde{\rho}_{ij}^{k+1|k} \prod_{l\in\sigma_{ijp}} \operatorname{sgn}\left(\tilde{\xi}_{ijl}^{k+1|k}\right). \tag{4.18}$$

Since ξ_{ij} and ξ_{il} of (4.15) have double indices, the difference $\xi_{il} - \xi_{ij}$ has a triple index ijl. To simplify this, the i and j indices are combined into a new i index, and the l index becomes the new j index. While this reindexing is not strictly necessary, it prevents us from having to keep adding new indices after every time propagation step. Furthermore, simplifying g and reindexing returns the structure of $\bar{f}_{\boldsymbol{X}_{k+1}|\boldsymbol{Y}_k}$ to the recursive form that we assumed at step $k|k-1$. Each of the $N^{k|k-1}$ terms of the integrand spawns $M_i^{k|k-1} + 1$ subterms, so the total number of terms at step $k+1|k$ becomes

$$\tilde{N}^{k+1|k} = \sum_{i=1}^{N^{k|k-1}} \left(M_i^{k|k-1} + 1\right), \tag{4.19}$$

with each term having $M_i^{k|k-1} + 1$ elements. Correspondingly, each $\tilde{\xi}_{ijl}^{k+1|k}$ becomes the new $\tilde{\xi}_{ij}^{k+1|k}$.

4.5. Special cases and term combination at $\boldsymbol{k+1|k}$. After the coefficient functions have been transformed into the basis form, several implementation considerations must be addressed. Some hyperplanes, as defined when the arguments of the sign functions equal zero, may become equal to another hyperplane, while other hyperplanes may disappear altogether, i.e., $\theta = 0$. These are special cases which result in a reduction in elements and thus the number of terms in g, leading to a reshuffle of parameters. After the special cases are resolved, terms with the same exponentials can be combined. At this point, the parameters lose the tilde and become $N^{k+1|k}, P_i^{k+1|k}, M_i^{k+1|k}, \rho_{ij}^{k+1|k}, \xi_{ij}^{k+1|k}$, and $\eta_{ij}^{k+1|k}$.

4.6. The ucpdf at $k+1|k$. Finally, we state the ucpdf at $k+1|k$ as

$$\bar{f}_{\boldsymbol{X}_{k+1}|\boldsymbol{Y}_k} = \sum_{i=1}^{N_i^{k+1|k}} \bar{g}_i^{k+1|k} \bar{\epsilon}_i^{k+1|k}, \tag{4.20}$$

where

$$\bar{g}_i^{k+1|k} = \bar{\rho}_{i0}^{k+1|k} + \sum_{j=1}^{P_i^{k+1|k}} \bar{\rho}_{ij}^{k+1|k} \prod_{l\in\sigma_{ij}} \operatorname{sgn}\left(\xi_{il}^{k+1|k}\right) \tag{4.21}$$

and

$$\bar{\epsilon}_i^{k+1|k} = \exp\left(-\sum_{j=1}^{M_i^{k+1|k}} \eta_{ij}^{k+1|k} \left|\xi_{ij}^{k+1|k}\right|\right), \tag{4.22}$$

where

$$\xi_{ij}^{k+1|k} = \psi_{ij}^{k+1|k} + \theta_{ij}^{k+1|k} \boldsymbol{x}_{k+1}, \tag{4.23}$$

$N^{k+1|k}$ is the number of terms, $M_i^{k+1|k}$ is the number of elements of term i, $P_i^{k+1|k}$ is the number of terms in $g_i^{k+1|k}$, and σ_{ij} is the set of indices of sign functions associated with term j of $g_i^{k+1|k}$ at step $k+1|k$. Thus, we've shown by induction that the update and propagation algorithm is recursive and preserves the underlying structure for $\bar{f}_{\boldsymbol{X}_k|\boldsymbol{Y}_{k-1}}$ in (4.1).

5. Mean and variance in $\mathbb{R}^n$. To determine the mean and variance of $\boldsymbol{X}$ given $\boldsymbol{Y}$, we first normalize $\bar{f}_{X|Y}$ and then compute the first and second moments. For this section, $\bar{f}_{\boldsymbol{X}|\boldsymbol{Y}}$ can be either a priori or a posteriori at any step k. Therefore, to simplify the presentation, the indices of the pdfs, used previously, are dropped in what follows. Instead of directly integrating to obtain the first two moments, we will derive them from the characteristic function of the ucpdf. The benefit of using characteristic functions is that one need only perform n integrations, followed by two relatively simple differentiations. In contrast, direct integration involves involves n integrations as well as two additional complicated integrations by parts [7, 6].

For $\boldsymbol{\nu}, \boldsymbol{x} \in \mathbb{R}^n$, where $\boldsymbol{\nu}$ is the spectral vector, the characteristic function of $\bar{f}_{X|Y}(\boldsymbol{x}|\boldsymbol{y})$ is the expectation of $e^{j\boldsymbol{\nu}^T\boldsymbol{x}}$, or

$$\bar{\phi}_{\boldsymbol{X}|\boldsymbol{Y}}(\boldsymbol{\nu}) = \int_{\mathbb{R}^n} e^{j\boldsymbol{\nu}^T\boldsymbol{x}} \bar{f}_{\boldsymbol{X}|\boldsymbol{Y}}(\boldsymbol{x}|\boldsymbol{y})\, d\boldsymbol{x}. \tag{5.1}$$

Evaluating (5.1) at $\boldsymbol{\nu} = \boldsymbol{0}$ gives the normalization factor

$$\left[\bar{\phi}_{\boldsymbol{X}|\boldsymbol{Y}}\right]_{\boldsymbol{\nu}=\boldsymbol{0}} = \int_{\mathbb{R}^n} \bar{f}_{\boldsymbol{X}|\boldsymbol{Y}}(\boldsymbol{x}|\boldsymbol{y})\, d\boldsymbol{x} = f_{\boldsymbol{Y}}. \tag{5.2}$$

Then, the normalized characteristic function is

$$\phi_{\boldsymbol{X}|\boldsymbol{Y}} = \frac{\bar{\phi}_{\boldsymbol{X}|\boldsymbol{Y}}}{f_{\boldsymbol{Y}}}. \tag{5.3}$$

Using (5.3), the mean and error variance are given by

$$\begin{aligned} \mu &= E\left[\boldsymbol{X}|\boldsymbol{Y}\right], \\ \mathrm{Var}(\boldsymbol{x}) &= E\left[\boldsymbol{X}\boldsymbol{X}^T|\boldsymbol{Y}\right] - E\left[\boldsymbol{X}|\boldsymbol{Y}\right]E\left[\boldsymbol{X}|\boldsymbol{Y}\right]^T, \end{aligned} \tag{5.4}$$

where the ith element of $E\left[\boldsymbol{X}|\boldsymbol{Y}\right]$ and the $i\ell$ element of the symmetric $E\left[\boldsymbol{X}\boldsymbol{X}^T|\boldsymbol{Y}\right]$ are

$$\begin{aligned} E\left[X_i|\boldsymbol{Y}\right] &= \left[\frac{1}{j}\frac{\partial \phi_{\boldsymbol{X}|\boldsymbol{Y}}(\boldsymbol{\nu})}{\partial \nu_i}\right]_{\boldsymbol{\nu}=\boldsymbol{0}}, \\ E\left[X_i X_\ell|\boldsymbol{Y}\right] &= \left[-\frac{\partial^2 \phi_{\boldsymbol{X}|\boldsymbol{Y}}(\boldsymbol{\nu})}{\partial \nu_i \partial \nu_\ell}\right]_{\boldsymbol{\nu}=\boldsymbol{0}}, \end{aligned} \tag{5.5}$$

respectively.

Note that we have abused the notation a little bit. Since we are not labeling the step number k, we use the subscript on the random variable X to indicate the element number instead. This should be clear in this context, even if it doesn't agree with the standard use of the subscript throughout this paper.

For $\boldsymbol{x} \in \mathbb{R}^n$, this requires n integrations as well as n single and $\sum_i^n i = \frac{n(n+1)}{2}$ double partial differentiations, though the differentiations can be done a priori. Although a numerical burden, it is less complicated than directly integrating to find the moments.

5.1. Characteristic function of ucpdf. To determine the characteristic function of $\bar{f}_{\boldsymbol{X}|\boldsymbol{Y}}$ in $\mathbb{R}^n$, we must integrate over $\mathbb{R}^n$, which means evaluating n successive integrals using the same integral formula that was used in previous sections. Consider the form $\bar{f}_{\boldsymbol{X}|\boldsymbol{Y}}$ to be

$$\bar{f}_{\boldsymbol{X}|\boldsymbol{Y}} = \sum_{i=1}^{N} \bar{g}_i(x) \exp\left(-\sum_{l=1}^{M_i} \eta_l \left|\psi_l + \theta_l \boldsymbol{x}\right|\right), \tag{5.6}$$

where, for M_i unique pairs $(\psi_l \in \mathbb{R}, \theta_l \in \mathbb{R}^{1\times n})$,

$$\bar{g}_i(x) = \bar{\rho}_{i0} + \sum_{q=1}^{P_i} \bar{\rho}_{iq} \prod_{l\in\sigma_{iq}} \mathrm{sgn}\left(\psi_l + \theta_l \boldsymbol{x}\right), \tag{5.7}$$

where g and σ_{iq} are unique subsets of $\{1,\ldots,M_i\}$. Note that when $M_i > n$, σ_{iq} can have at most n elements of $\{1,\ldots,M_i\}$. Using the generalized integral formula (3.22), (5.1) can be solved elementwise, and each element can be explicitly written as

$$
\begin{aligned}
\phi^i_{\boldsymbol{X}|\boldsymbol{Y}} &= \int_x e^{j\nu^T x}\bar{g}_i(x)\exp\left(-\sum_{l=1}^{M_i}\eta_l\left|\psi_l+\theta_l\boldsymbol{x}\right|\right)dx \\
&= \int_{x_1}\cdots\int_{x_n}\left(\rho_{i0}+\sum_{q=1}^{P_i}\rho_{iq}\prod_{l\in\sigma_q}\operatorname{sgn}\left(\psi_l+\theta_l\boldsymbol{x}\right)\right) \\
&\qquad\qquad\cdot\exp\left(-\sum_{l=1}^{M_i}\eta_l\left|\psi_l+\theta_l\boldsymbol{x}\right|+j\nu^T x\right)dx_1\cdots dx_n \\
&= \int_{x_1}\cdots\int_{x_n}\left(\rho_{i0}+\sum_{q=1}^{P_i}\rho_{iq}\prod_{l\in\sigma_q}\operatorname{sgn}\left(\psi_l+\theta_1x_1+\cdots+\theta_nx_n\right)\right) \\
&\quad\cdot\exp\left[-\sum_{l=1}^{M_i}\eta_l\left|\psi_l+\theta_{l1}x_1+\cdots+\theta_{ln}x_n\right|+j\left(\nu_1x_1+\cdots+\nu_nx_n\right)\right]dx_1\cdots dx_n.
\end{aligned}
\tag{5.8}
$$

Note that care must be taken to account for variables which are constant for one integration but are not constant for another. For example, x_1 is constant when integrating with respect to x_2. However, it is not constant in the subsequent integration with respect to x_1.

5.2. Normalization and moments from characteristic function in $\mathbb{R}^2$. Applying (5.8) to the two-dimensional case results in

$$
\bar{\phi}_{\boldsymbol{X}|\boldsymbol{Y}} = \sum_{i=1}^N \bar{\phi}^i_{\boldsymbol{X}|\boldsymbol{Y}} = \sum_{i=1}^N \bar{G}_i(\nu_1,\nu_2)\mathcal{E}_i(\nu_1,\nu_2),
\tag{5.9}
$$

where, after some involved algebra,

$$
\begin{aligned}
\bar{G}_i(\nu_1,\nu_2) &= \frac{\frac{a_{i1}}{a_{i2}+j\nu_2}-\frac{a_{i3}}{a_{i4}+j\nu_2}}{a_{i5}+j\nu_1+a_{i6}\cdot j\nu_2}-\frac{\frac{b_{i1}}{b_{i2}+j\nu_2}-\frac{b_{i3}}{b_{i4}+j\nu_2}}{b_{i5}+j\nu_1+b_{i6}\cdot j\nu_2}, \\
\mathcal{E}_i(\nu_1,\nu_2) &= \exp\left(c_{i1}\cdot j\nu_1+c_{i2}\cdot j\nu_2+c_{i3}\right),
\end{aligned}
\tag{5.10}
$$

and $a_{i1},\ldots,a_{i6}$, $b_{i1},\ldots,b_{i6}$, and $c_{i1},\ldots,c_{i3}$ are constants.

Applying (5.2) to (5.9), the normalization factor becomes

$$
f_{\boldsymbol{Y}} = \sum_{i=1}^N f^i_{\boldsymbol{Y}},
\tag{5.11}
$$

where

$$
f^i_{\boldsymbol{Y}} = \left[\bar{\phi}^i_{\boldsymbol{X}|\boldsymbol{Y}}\right]_{\boldsymbol{\nu}=\boldsymbol{0}} = \left(\frac{\frac{a_{i1}}{a_{i2}}-\frac{a_{i4}}{a_{i5}}}{a_{i7}}-\frac{\frac{b_{i1}}{b_{i2}}-\frac{b_{i4}}{b_{i5}}}{b_{i7}}\right)\exp\left(c_{i3}\right).
\tag{5.12}
$$

Using (5.11), the *normalized* characteristic function becomes

$$
\begin{aligned}
\phi_{\boldsymbol{X}|\boldsymbol{Y}} &= \frac{\sum_{i=1}^N\bar{\phi}^i_{\boldsymbol{X}|\boldsymbol{Y}}}{f_{\boldsymbol{Y}}} = \sum_{i=1}^N\frac{\bar{G}_i(\nu_1,\nu_2)}{f_{\boldsymbol{Y}}}\cdot\mathcal{E}_i(\nu_1,\nu_2) \\
&\triangleq \sum_{i=1}^N G_i(\nu_1,\nu_2)\cdot\mathcal{E}_i(\nu_1,\nu_2).
\end{aligned}
\tag{5.13}
$$

The ith term of the first two moments in $\mathbb{R}^2$ are

$$E^i[\boldsymbol{X}] = \begin{bmatrix} \frac{1}{j}\frac{\partial\phi^i}{\partial\nu_1} \\ \frac{1}{j}\frac{\partial\phi^i}{\partial\nu_2} \end{bmatrix}_{\boldsymbol{\nu}=\boldsymbol{0}}, \tag{5.14}$$

$$E^i\left[\boldsymbol{X}\boldsymbol{X}^T\right] = \begin{bmatrix} -\frac{\partial^2\phi^i}{\partial\nu_1^2} & -\frac{\partial^2\phi^i}{\partial\nu_1\partial\nu_2} \\ -\frac{\partial^2\phi}{\partial\nu_1\partial\nu_2} & -\frac{\partial^2\phi}{\partial\nu_2^2} \end{bmatrix}_{\boldsymbol{\nu}=\boldsymbol{0}}.$$

The partial derivatives are somewhat long due to multiple implementations of the product and quotient rules. However, they are straightforward and the expressions are omitted for brevity.

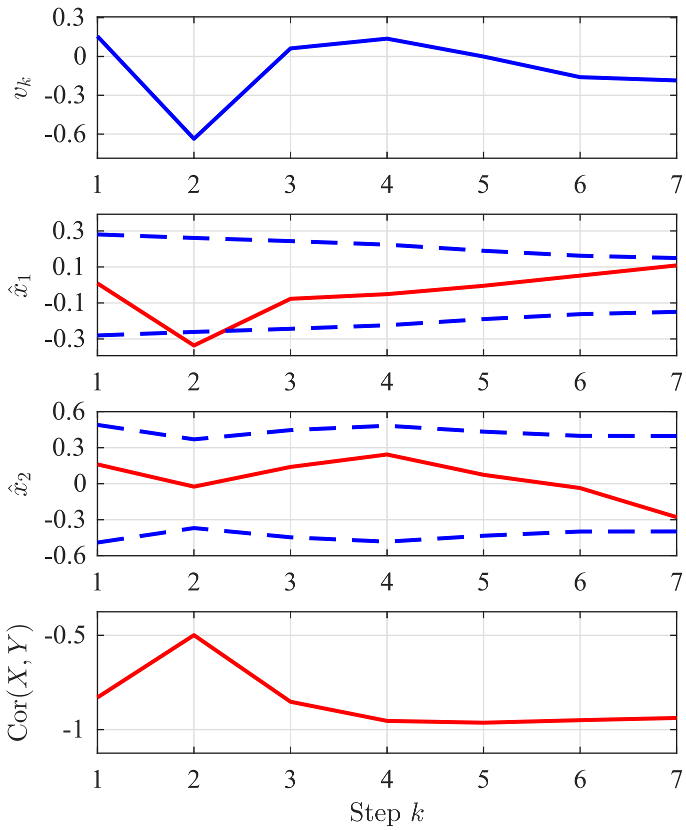

FIG. 4. *Estimation errors for seven steps in $\mathbb{R}^2$ for $\alpha = 0.3, \beta = 0.01, \gamma = 0.1$.*

6. Numerical example. A two-state example of the Laplace estimator was implemented in MATLAB to illustrate the theory developed in section 4. For the stochastic system of (2.1) with system parameters, initial conditions, and noise parameters given in (3.19), the conditional mean and conditional error variance defined in (5.5) are computed.

Figure 4 shows the results for a seven-step simulation where we can see that the covariance changes as a function of the measurement. In addition, the response to the large jump in the measurement at $k = 2$ is rather muted, despite the fact that $z_k = x_1 + 0.5x_2$.

6.1. Incremental enumeration. The algorithm for transforming the coefficient functions, g, from the nested, fractional form of the integral formula to a sum of basis sign functions is described in Appendix B. In order to enumerate the faces of the hyperplane arrangements defined by the sign functions in g, we first experimented with the reverse search algorithm by Avis and Fukuda in [1]. However, that algorithm had some numerical issues and was particularly slow. Instead, we use the algorithms developed by Rada and Cerný in [20], along with linear program solvers by Gurobi to enumerate the faces. The coefficients of g are then found by solving a linear equation using standard solvers.

6.2. Computational aspects. We analyze the growth in the quantity of parameters needed to define the cpdfs. As shown in (4.19), the number of elements in the exponential increases by 1 every step, so it grows as k. In addition, each term at step k in the a posteriori cpdf spawns the number of elements plus one additional term, so the total number of terms grows as $k+2$ factorial. As shown in Theorem 3.1, due to the basis functions, the worst-case coefficient function grows as $\sum_{j=0}^{n} \binom{k}{j}$, or k^n. Therefore, the worst-case number of parameters needed to define the a posteriori cpdf grows as $(k + 2)! \cdot k^{n+1}$. In practice, we do not approach the worst case due to combining terms enabled by Theorem 3.1 and special cases discussed in section 4.5.

Practical implementation of the Laplace estimator may require a moving fixed window of data which bounds the computation. The parallel structure of the pdfs can be exploited by use of GPU-assisted architectures, such as CUDA. Efficient computational architectures will enable comparison with current approximate algorithms.

7. Conclusions. A recursive algorithm for determining the cpdf given the measurement history of an n-dimensional linear dynamic system with additive Laplace noise is determined. The unnormalized conditional pdf of the state conditioned on the measurement history was propagated and updated analytically and recursively. Unlike for approximate Laplace estimation techniques, expectations can be computed directly using the cpdf, which allows for construction of L_1 cost functions and use in optimal control schemes [5].

The ucpdf is composed of a growing sum of terms, where each term is composed of a product of an exponential, whose argument is the sum of absolute values of affine functions of $\boldsymbol{x}$, and a coefficient function g, composed of signs of the same affine functions. On each face of the hyperplane arrangement, g is constant. To construct the recursion, it is necessary to restructure the functional form of g by constructing a basis, which also allows some terms to sum. The structure of the basis required a generalization of an integral formula, used in the propagation step and in constructing the characteristic function from which the conditional mean and conditional error variance are evaluated. It it shown numerically that the conditional error variance changes with the measurements.

Appendix A. Key integral formula. Appendix B of [12] gives the solution for

$$I = \int_{-\infty}^{\infty} g\left(\sum_{i=1}^{n} \varrho_i \operatorname{sgn}(\xi_i - \eta)\right) \exp\left(-\sum_{i=1}^{n} \rho_i \left|\xi_i - \eta\right| + j\nu\eta\right) d\eta, \tag{A.1}$$

where g is an explicit function of a sum of sign functions. We extend the solution to include g as any function of the n sign functions corresponding to ξ in the exponential, i.e.,

$$I = \int_{-\infty}^{\infty} g\left(\eta\right) \exp\left(-\sum_{l=1}^{n} \rho_l \left|\xi_l - \eta\right| + j\nu\eta\right) d\eta, \tag{A.2}$$

where

$$g(\eta) = g\left(\operatorname{sgn}\left(\xi_1 - \eta\right), \ldots, \operatorname{sgn}\left(\xi_n - \eta\right)\right). \tag{A.3}$$

As in the original derivation, $\operatorname{sgn}\left(\xi_\ell - \eta\right)$ is constant on the interval $(\xi_i, \xi_{i+1}]$ such that

$$\operatorname{sgn}\left(\xi_\ell - \eta\right) \triangleq s_i^\ell = \begin{cases} \operatorname{sgn}\left(\xi_\ell - \xi_i\right), & i \neq \ell, \\ -1, & i = \ell. \end{cases} \tag{A.4}$$

The original derivation in [12] is valid for the general $g(\eta)$ until substituting s_i^ℓ for s_{i-1}^l in the left term. It is shown that $s_{i-1}^l = s_i^\ell$ except for when $i = \ell$, where $s_{i=1}^\ell = 1$ instead of -1. This leads to the equation

$$\sum_{i=1}^{n} \rho_i s_{i-1}^\ell = \rho_i + \sum_{\substack{\ell=1 \\ \ell \neq i}}^{n} \rho_i s_i^\ell, \tag{A.5}$$

which is the common argument in the final expression of the integral formula. However, (A.5) is only valid for a sum of sign functions. Therefore, the denominator is the same as in [12], but the numerator requires us to identify when $i = \ell$ and evaluate $s_i^\ell = 1$. Therefore, the solution is

$$I = \sum_{i=1}^{n} \bar{g}_i \exp\left(-\sum_{\ell=1}^{n} \rho_\ell (\xi_\ell - \xi_i) s_i^\ell + j\nu\xi_i\right), \tag{A.6}$$

where

$$\bar{g}_i = \frac{g\left(\xi_i\right)^\dagger}{j\nu + \rho_i + \sum\limits_{\substack{l=1 \\ l \neq i}}^{n} \rho_\ell s_i^\ell} - \frac{g\left(\xi_i\right)}{j\nu - \rho_i + \sum\limits_{\substack{l=1 \\ l \neq i}}^{n} \rho_\ell s_i^\ell}, \tag{A.7}$$

where $g^\dagger$ indicates that every instance of $s_i^\ell = 1$ when $i = \ell$. It is clear that the integral formula in [12] is a special case of (A.6) and (A.7).

Appendix B. Algorithm for finding coefficients of the basis of the g's in $\mathbb{R}^2$. The coefficient function g is piecewise constant on each of n-dimensional faces defined by the hyperplane arrangement associated with the arguments of its sign functions. Therefore, we wish to evaluate each sign function on each face, which can then be used to evaluate both g and the basis functions from (4.18). We know from Theorem 3.1 that all of the unique combinations of products of at most n sign functions present in g form a basis for g. With the value of g and sign basis known, we can rearrange (4.18) into a linear equation to solve for the coefficients ρ.

For simplicity, we will show the algorithm for the $\mathbb{R}^2$ case, but it easily extends to n dimensions. Let us evaluate $g : \mathbb{R}^2 \to \mathbb{R}$, composed of m sign functions on each of N faces, and arrange the values into the vector

$$y = \begin{bmatrix} g_1 \\ g_2 \\ \vdots \\ g_N \end{bmatrix}. \tag{B.1}$$

We then evaluate the basis functions on each face and arrange them into the matrix

$$S = \begin{bmatrix} 1 & s_{1,1} & \cdots & s_{1,2} & \cdots & s_{1,1}s_{1,2} & \cdots & s_{1,m-1}s_{1,m} \\ 1 & s_{2,1} & \cdots & s_{2,2} & \cdots & s_{2,1}s_{2,2} & \cdots & s_{2,m-1}s_{2,m} \\ \vdots & \vdots & \ddots & \vdots & \ddots & \vdots & \ddots & \vdots \\ 1 & s_{N,1} & \cdots & s_{N,2} & \cdots & s_{N,1}s_{N,2} & \cdots & s_{N,m-1}s_{N,m} \end{bmatrix}. \tag{B.2}$$

The samples (B.1) and basis (B.2) are related as

$$y = S\rho, \tag{B.3}$$

where

$$\rho = \begin{bmatrix} \rho_0 & \rho_1 & \rho_2 & \cdots & \rho_{N_b} \end{bmatrix}^T, \tag{B.4}$$

where N is the number of distinct polytopes in $\mathbb{R}^n$ generated by the m sign functions. Before we solve (B.3), we will show that it will always have at least one solution.

Consider the hyperplane arrangement defined in Theorem 3.1, and let N be the number of faces of $\mathcal{A}$ and be bounded by

$$N \leq \sum_{k=0}^{n} \binom{m}{k}. \tag{B.5}$$

From Theorem 3.1, for every constant-valued region $F_j, j = 1, \ldots, N$, there exists $\rho_0, \ldots, \rho_P$ such that for every $\boldsymbol{x}_j \in F_j$, $g(\boldsymbol{x}_j)$ has the form of (3.15). Since

$$P(m,n) = \sum_{k=0}^{n} \binom{m}{k}, \tag{B.6}$$

$N \leq P(m)$. Observe that N is the number of rows and $P(m,n)$ is the number of columns of S. From Corollary 3.2, the rows of S form a basis for any $g(\boldsymbol{x})$ and are thus independent. Consequently, since S has full row rank, there exists at least one solution to (B.3). A particular solution is the least-norm solution, or

$$\hat{\rho}_{\ln} = S^T \left(SS^T\right)^{-1} y, \tag{B.7}$$

which is what we get when we use the MATLAB `pinv` function. Note that using the left matrix divide, or backslash (`A\b`), to solve this equation yields the solution with the greatest number of zero elements instead of the least-norm.

REFERENCES

[1] D. Avis and K. Fukuda, *Reverse search for enumeration*, Discrete Appl. Math., 65 (1996), pp. 21–46.

[2] M. C. Bryson, *Heavy-tailed distributions: Properties and tests*, Technometrics, 16 (1974), pp. 61–68, https://doi.org/10.1080/00401706.1974.10489150.

[3] R. E. Carrillo, K. E. Barner, and T. C. Aysal, *Robust sampling and reconstruction methods for sparse signals in the presence of impulsive noise*, IEEE J. Sel. Top. Signal Process., 4 (2010), pp. 392–408, https://doi.org/10.1109/JSTSP.2009.2039177.

[4] N. Duong, M. Idan, R. Pinchasi, and J. Speyer, *A note on hyper-plane arrangements in* $\mathbb{R}^d$, Discrete Math. Lett., 7 (2021), pp. 79–85, https://doi.org/10.47443/dml.2021.0048.

[5] N. Duong, J. Speyer, and M. Idan, *Laplace controller for linear scalar systems*, in Proceedings of the 27th Mediterranean Conference on Control and Automation (MED), Akko, Israel, 2019, pp. 334–339.

[6] N. Duong, J. Speyer, and M. Idan, *Laplace estimation for linear scalar systems*, J. IFAC, 144 (2022), 110301.

[7] N. Duong, J. Speyer, J. Yoneyama, and M. Idan, *Laplace estimator for linear scalar systems*, in Proceedings of the 57th IEEE Conference on Decision and Control, Miami, FL, 2018.

[8] F. Farokhi, J. Milosevic, and H. Sandberg, *Optimal state estimation with measurements corrupted by Laplace noise*, in Proceedings of the 2016 IEEE 55th Conference on Decision and Control (CDC), 2016, pp. 302–307.

[9] J. Fernández, J. L. Speyer, and M. Idan, *Stochastic estimation for two-state linear dynamic systems with additive Cauchy noises*, IEEE Trans. Automat. Control, 60 (2015), pp. 3367–3372, https://doi.org/10.1109/TAC.2015.2422478.

[10] M. Idan and J. L. Speyer, *Cauchy estimation for linear scalar systems*, IEEE Trans. Automat. Control, 55 (2010), pp. 1329–1342.

[11] M. Idan and J. L. Speyer, *State estimation for linear scalar dynamic systems with additive Cauchy noises: Characteristic function approach*, SIAM J. Control Optim., 50 (2012), pp. 1971–1994, https://doi.org/10.1137/110831362.

[12] M. Idan and J. L. Speyer, *Multivariate Cauchy estimator with scalar measurent and process noises*, SIAM J. Control Optim., 52 (2014), pp. 1108–1141, https://doi.org/10.1137/120891897.

[13] O. Karakus, P. Mayo, and A. Achim, *Convergence guarantees for non-convex optimisation with Cauchy-based penalties*, IEEE Trans. Signal Process., 68 (2020), pp. 6159–6170, https://doi.org/10.1109/TSP.2020.3032231.

[14] P. Kozierski, T. Sadalla, A. Owczarkowski, and S. Drgas, *Particle filter in multidimensional systems*, in Proceedings of the 2016 21st International Conference on Methods and Models in Automation and Robotics (MMAR), 2016, pp. 806–810.

[15] E. E. Kuruoglu, W. J. Fitzgerald, and P. J. W. Rayner, *Near optimal detection of signals in impulsive noise modeled with a symmetric /SPL alpha/-stable distribution*, IEEE Commun. Lett., 2 (1998), pp. 282–284.

[16] B. N. M. Laska, M. Bolic, and R. A. Goubran, *Particle filter enhancement of speech spectral amplitudes*, IEEE Trans. Audio Speech Lang. Process., 18 (2010), pp. 2155–2167.

[17] M. Linden, *Estimating the distribution of volatility of realized stock returns and exchange rate changes*, Phys. A, 352 (2005), pp. 573–583, https://doi.org/10.1016/j.physa.2004.12.024.

[18] C. Musso, P. Bui Quang, and F. Le Gland, *Introducing the Laplace approximation in particle filtering*, in Proceedings of the 14th International Conference on Information Fusion, 2011, pp. 1–8.

[19] H. Rabbani, M. Vafadust, and S. Gazor, *Image denoising based on a mixture of Laplace distributions with local parameters in complex wavelet domain*, in Proceedings of the 2006 International Conference on Image Processing, 2006, pp. 2597–2600.

[20] M. Rada and M. Cerný, *A new algorithm for enumeration of cells of hyperplane arrangements and a comparison with Avis and Fukuda's reverse search*, SIAM J. Discrete. Math., 32 (2018), pp. 455–473, https://doi.org/10.1137/15M1027930.

[21] I. W. Selesnick, *The estimation of Laplace random vectors in additive white Gaussian noise*, IEEE Trans. Signal Process., 56 (2008), pp. 3482–3496.

[22] J. Speyer, J. Yoneyama, N. Duong, and M. Idan, *Laplace one-step controller for linear scalar systems*, in Proceedings of the 2018 European Control Conference, Limassol, Cyprus, 2018, pp. 2703–2707.

[23] J. L. Speyer and W. H. Chung, *Stochastic Processes, Estimation, and Control*, Adv. Des. Control 17, SIAM, Philadelphia, 2008, https://doi.org/10.1137/1.9780898718591.